Spectrochimica Acta Part A: Molecular and Biomolecular Spectroscopy 131 (2014) 490–496

Contents lists available at ScienceDirect

Spectrochimica Acta Part A: Molecular and Biomolecular Spectroscopy

journal homepage: www.elsevier.com/locate/saa

Synthesis, spectral and catalytic dehydrogenation studies of ruthenium complexes containing NO bidentate ligands

A.F. Shoair, A.A. El-Bindary *

Chemistry Department, Faculty of Science, Damietta University, 34517 Damietta, Egypt

HIGHLIGHTS

- Ruthenium mononuclear complexes containing NO bidentate ligands.
- The complexes are characterized by different spectroscopic techniques.
- Ruthenium complexes are used as catalysts dehydrogenation of different amines to their respective nitriles.
- The relative stabilities of the oxidation and reduction states are examined electrochemically.

GRAPHICAL ABSTRACT

ESR spectrum of $[Ru^{III}Cl(2\text{-aph})_2(H_2O)]$ (**2a**) in DMF/toluene at 77 K.

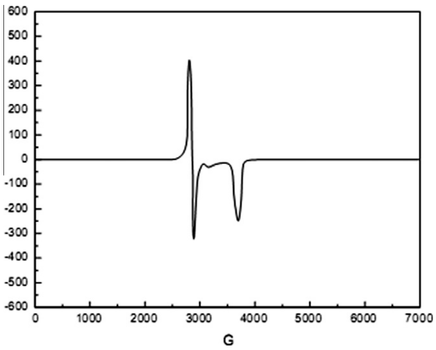

ARTICLE INFO

Article history:
Received 21 February 2014
Received in revised form 3 April 2014
Accepted 14 April 2014
Available online 30 April 2014

Keywords:
Ruthenium
NO bidentate ligands
Catalytic dehydrogenation
Electrochemistry

ABSTRACT

The synthesis and characterization of ruthenium mononuclear complexes containing NO bidentate ligands are reported. The complexes cis-$[Ru^{II}(bpy)_2L](PF_6)_n$ (**1a–c**), $[Ru^{III}Cl(L)_2(H_2O)]$ (**2a–b**) and $[Ru^{III}Cl_2(L)_2]Cl$ (**2c**) were prepared by the reaction of cis-$[Ru^{II}Cl_2(bpy)_2]\cdot 2H_2O$ (bpy = 2,2′-bipyridine) and/or $RuCl_3\cdot nH_2O$ with the Ligands: 2-aminophenol (2-aph), 8-hydroxyquinoline (8-hq) and 4-aminoantipyrine (4-apy). These complexes were characterized by elemental analysis, spectroscopic (IR, UV–Vis, ^1H NMR, ESR) and magnetic susceptibility measurements. The ligand field parameters, Δ_o (splitting parameter), B (Racah parameter of interelectronic repulsion), and β (nephelauxetic ratio) were calculated. The redox properties were also investigated electrochemically by cyclic voltammetry. The complexes cis-$[Ru^{II}(bpy)_2(8\text{-hq})](PF_6)_2$ (**1b**) and $[Ru^{III}Cl(8\text{-hq})_2(H_2O)]$ (**2b**) have been investigated in conjunction with *N*-methylmorpholine-*N*-oxide (NMO) as co-oxidant for the catalytic dehydrogenation of benzyl amine, *p*-methyl benzylamine and *p*-nitrobenzylamine to their respective nitriles.

Introduction

Ruthenium complexes have been extensively studied, particularly those containing 2,2′-bipyridine or NO bidentate ligands. These complexes have attracted great attention in fields of solar energy conversion, artificial photosynthesis and optical sensing, due to their favorable photophysical properties, excited state reactivities and chemical stabilities [1–4]. In addition, ruthenium complexes have been proven to be a good catalyst for the oxidation of organic compounds [5–8]. The dehydrogenation of primary amines plays an important role in the synthesis of nitriles. However, the development of new oxidative processes continues to draw an attention in spite of the availability of numerous oxidizing agents [9,10]. Nitriles are useful intermediates in the synthesis of biologically active compounds and pharmaceutical substances [11]. Therefore,

---

* Corresponding author. Tel.: +20 1114266996; fax: +20 572403868.
E-mail address: abindary@yahoo.com (A.A. El-Bindary).

http://dx.doi.org/10.1016/j.saa.2014.04.132
1386-1425/© 2014 Elsevier B.V. All rights reserved.

the development of efficient catalytic systems for the oxidative dehydrogenation of primary aromatic amines to nitriles has attracted much attention [12,13]. As a part of our efforts to develop new ruthenium(II)/(III) complexes containing inexpensive ligands [14–17] and their applications as catalysts [18,19], we report herein the synthesis and characterization of ruthenium complexes; cis-[$Ru^{II}(bpy)_2L](PF_6)_n$ (**1a–c**), [$Ru^{III}Cl(L)_2(H_2O)$] (**2a–b**) and [$Ru^{III}Cl_2(L)_2$]Cl (**2c**) by the reaction of cis-[$Ru^{II}Cl_2(bpy)_2]\cdot 2H_2O$ (bpy = 2,2′-bipyridine) and/or $RuCl_3\cdot nH_2O$ with the ligands 2-aminophenol (2-aph), 8-hydroxyquinoline (8-hq) and 4-aminoantipyrine (4-apy). The catalytic activities of the characterized complexes; cis-[$Ru^{II}(bpy)_2$(8-hq)]$(PF_6)_2$ (**1b**) and [$Ru^{III}Cl$(8-hq)$_2$(H_2O)] (**2b**) towards dehydrogenation of benzyl amine, *p*-methylbenzylamine and *p*-nitrobenzylamine to their respective nitriles in the presence of *N*-methylmorpholine-*N*-oxide (NMO) as co-oxidant were investigated at room temperature. The relative stabilities of the oxidation and reduction states are examined electrochemically.

Experimental

Chemicals and physical measurements

All chemicals and solvents were of analytical grade and used without further purification. Ruthenium chloride, 2-aminophenol, 8-hydroxyquinoline and 4-aminoantipyrine were purchased from Sigma–Aldrich Chemicals Company (USA). Microanalyses were performed using a Perkin–Elmer CHN 2400 microanalysis unit at Cairo University (Cairo, Egypt). The IR spectra were recorded as KBr discs in the 4000–400 cm^{-1} range on a JASCO 410 spectrophotometer. The electronic absorption spectra were obtained in DMF solution on a Perkin–Elmer Lambada 2 spectrophotometer. Magnetic measurements were carried out at room temperature using Gouy's method, employing $Hg[Co(SCN)_4]$ for calibration purpose and were corrected for diamagnetism by using Pascal's constant. ^1H NMR spectra in d_6-DMSO were recorded on a Varian Unit plus 300 MHz model using TMS as an internal standard. ESR measurements of the polycrystalline samples were recorded on a Bruker ECS 106 EPR spectrometer using a quartz Dewar vessel at room temperature (College of Science, Department of Chemistry, Tamkang University, Taiwan). All spectra were calibrated with DPPH ($g = 2.0027$). The electrochemical behavior of the complexes was studied using an electrochemical analyzer CH1 610A (HCH Instrument). The electrochemical cell assembly consists of Pt wire as working electrode, a Pt wire auxiliary electrode and Ag/AgCl, KCl (3.0 mol L^{-1}) as a reference electrode. The reference electrode was separated from the bulk solution by a fitted-glass bridge filled with the solvent/supporting electrolyte mixture. Tetrabutylammonium chloride (TBAC) was used as the supporting electrolyte and the scan rate used was 50 mV s^{-1} in dry DMF under nitrogen atmosphere.

Preparation of cis-[$RuCl_2(bpy)_2]\cdot 2H_2O$ complex

The complex cis-[$Ru^{II}Cl_2(bpy)_2]\cdot 2H_2O$ (where bpy = 2,2′-bipyridine) was prepared using the method suggested by Sullivan et al. [20].

Preparation of ruthenium(II) complexes (*1a–c*)

The complexes cis-[$Ru^{II}(bpy)_2$(2-aph)](PF_6) (**1a**) and cis-[$Ru^{II}(bpy)_2$(8-hq)](PF_6) (**1b**) and cis-[$Ru^{II}(bpy)_2$(4-apy)]$(PF_6)_2$ (**1c**) (Scheme 1) were prepared by adding an methanolic triethylamine (10%, 0.21 mmol, 0.29 mL) followed by the ligand (1.2 mmol) in methanol (5 mL) to a suspension of cis-[$RuCl_2(bpy)_2]\cdot 2H_2O$ (104 mg, 0.2 mmol) in aqueous methanol (5 mL). The reaction

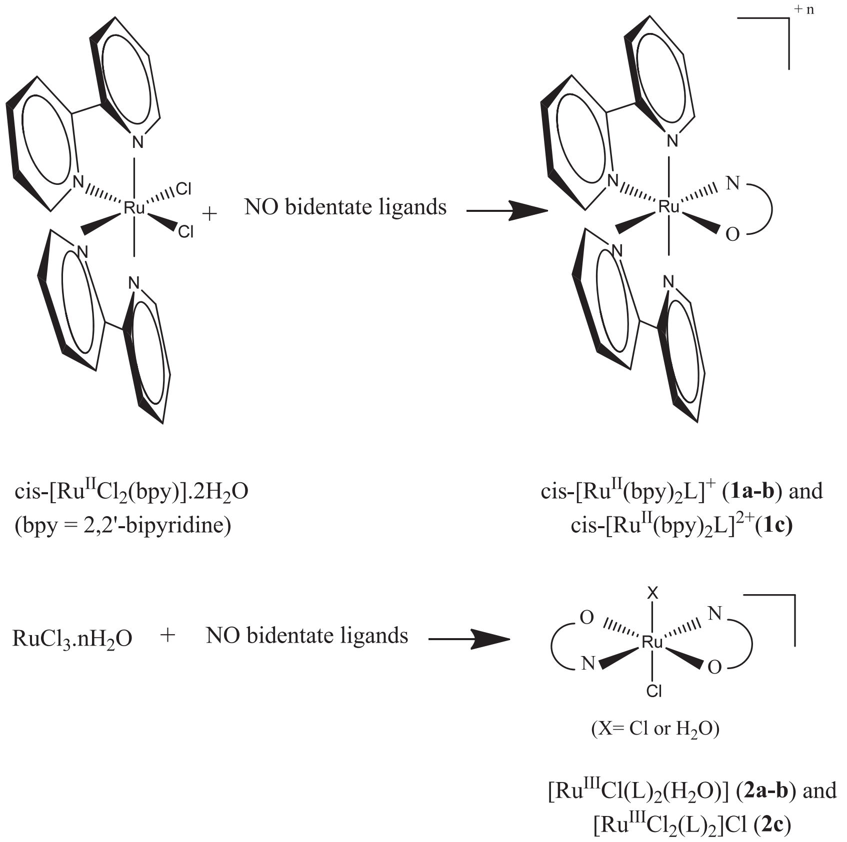

Scheme 1. The proposed structures of cis-[$Ru^{II}(bpy)_2L]^+$ (**1a–b**), cis-[$Ru^{II}(bpy)_2L]^{2+}$ (**1c**) and [$Ru^{III}Cl(L)_2(H_2O)$] (**2a–b**) [$Ru^{III}Cl_2(L)_2$]Cl (**2c**) complexes [ligands (L) = 2-aminophenolate (2-aph), 8-hydroxyquinolate (8-hq) and 4-aminoantipyrine (4-apy)].

mixture was refluxed under nitrogen for 3 h during which the initial dark brown color turned to dark red. The reaction was cooled to room temperature and methanol was evaporated under reduced pressure and the aqueous solution filtered through a sintered glass. The complexes were precipitated by addition of saturated aqueous solution of NH_4PF_6 (0.1 mg in 3 mL H_2O). The resulting solid complexes were collected by filtration, washed by water and dried in vacuuo over anhydrous $CaCl_2$. The yield was (70–75%).

Elemental analysis for cis-$[Ru^{II}(bpy)_2(2\text{-aph})](PF_6)$ (**1a**):

Calcd (%) for $C_{26}H_{22}N_5OPF_6Ru$ (MW = 666.49): C, 46.81; H, 3.30; N, 10.5; Found: C, 46.41; H, 3.40; N, 10.2. Selected IR bands (KBr, cm^{-1}): 3430b υ(OH), 3285m $υ_s(NH_2)$, 3325m $υ_{as}(NH_2)$, 465 υ(Ru—O), 437 υ(Ru—N).

Elemental analysis for cis-$[Ru^{II}(bpy)_2(8\text{-hq})](PF_6)$ (**1b**):

Calcd (%) for $C_{29}H_{22}N_5OPF_6Ru$ (MW = 703.52): C, 49.46; H, 3.12; N, 9.94; Found: C, 49.92; H, 3.10; N, 9.75. Selected IR bands (KBr, cm^{-1}): 3390b υ(OH), 455w υ(Ru—O), 435 υ(Ru—N).

Elemental analysis for cis-$[Ru^{II}(bpy)_2(4\text{-apy})](PF_6)_2$ (**1c**):

Calcd (%) for $C_{32}H_{29}N_7OP_2F_{12}Ru$ (MW = 905.60): C, 41.07; H, 3.20; N, 10.82; Found: C, 41.27; H, 3.40; N, 11.22. Selected IR bands (KBr, cm^{-1}): 3260m $υ_s(NH_2)$, 3320m $υ_{as}(NH_2)$, 1660m υ(C=O), 459 υ(Ru—O), 442 υ(Ru—N).

*Preparation of ruthenium(III) complexes (**2a–c**)*

The complexes $[Ru^{III}Cl(2\text{-aph})_2(H_2O)]$ (**2a**) $[Ru^{III}Cl(8\text{-hq})_2(H_2O)]$ (**2b**) and $[Ru^{III}Cl_2(4\text{-apy})_2]Cl$ (**2c**) (Scheme 1) were prepared by dissolving $RuCl_3{\cdot}nH_2O$ (100 mg, 0.4 mmol) in ethanol (10 mL) under reflux until the initial black color turned into green and an ethanolic solution of the ligand (2 mmol) was added. The reaction mixture was refluxed for 3 h. The resulting olive-green solid complexes were collected by filtration, washed by hot ethanol and dried in vacuuo over anhydrous $CaCl_2$. The yield was (60–70%).

Elemental analysis for $[Ru^{III}Cl(2\text{-aph})_2(H_2O)]$ (**2a**):

Calcd (%) for $C_{12}H_{14}N_2O_3ClRu$ (MW = 370.76): C, 38.84; H, 3.77; N, 7.55; Found: C, 39.54; H, 3.97; N, 7.75. Selected IR bands (KBr, cm^{-1}): 3440b υ(OH), 3280m $υ_s(NH_2)$, 3320m $υ_{as}(NH_2)$, 329vs (Ru—Cl), 455 υ(Ru—O), 450 υ(Ru—N).

Elemental analysis for $[Ru^{III}Cl(8\text{-hq})_2(H_2O)]$ (**2b**):

Calcd (%) for $C_{18}H_{14}N_2O_3ClRu$ (MW = 442.82): C, 48.78; H, 3.16; N, 6.32; Found: C, 49.68; H, 3.46; N, 6.72. Selected IR bands (KBr, cm^{-1}): 3460b υ(OH), 324vs υ(Ru—Cl), 460 υ(Ru—O), 444 υ(Ru—N).

Elemental analysis for $[Ru^{III}Cl_2(4\text{-apy})_2]Cl$ (**2c**):

Calcd (%) for $C_{22}H_{26}N_6O_2Cl_3Ru$ (MW = 613.98): C, 42.99; H, 4.23; N, 13.68; Found: C, 43.11; H, 4.45; N, 13.78. Selected IR bands (KBr, cm^{-1}): 3260m $υ_s(NH_2)$, 3315m $υ_{as}(NH_2)$, 1670m υ(C=O), 330vs υ(Ru—Cl), 455w υ(Ru—O), 445 υ(Ru—N).

Catalytic dehydrogenation of benzylamine to benzonitrile

Catalytic dehydrogenation of benzylamine (2 mmol) was carried out using (0.01 mmol, 10 mL DMF) of cis-$[Ru^{II}(bpy)_2(8\text{-hq})](PF_6)$ (**1b**) or $[Ru^{III}Cl(8\text{-hq})_2(H_2O)]$ (**2b**) complexes as a catalyst and *N*-methylmorpholine-*N*-oxide (NMO) (3 mmol, DMF) as co-oxidant in refluxing and stirring condition for 3 h at room temperature [7,20]. The mixture was taken up in diethylether, and filtered through a bed of silica gel. The produced benzonitrile was weighed and identified by comparing the IR and melting points of the produced benzonitriles with an authentic sample.

Results and discussion

All the complexes were air stable, non-hygroscopic solids, which decomposed at high temperature and were found to be insoluble in common organic solvents. The stoichiometries of the complexes have been deduced from their elemental analysis results. The ligands are bidentate and coordinate through oxygen atom of deprotonated hydroxyl group and nitrogen atom of the amino group. However, the complexes cis-$[Ru^{II}(bpy)_2L](PF_6)$ (**1a–b**) and cis-$[Ru^{II}(bpy)_2L](PF_6)_2$ **(1c)** have C_1-symmetry while the complexes, $[Ru^{III}Cl(L)_2(H_2O)]$ (**2a–b**) $[Ru^{III}Cl_2(L)_2]Cl$ (**2c**) have a D_{2h}-symmetry. The magnetic susceptibility measurements show that the complexes **(1a–c)** are diamagnetic (low spin d^6 S = 0) while the complexes **(2a–c)** are paramagnetic (μ_{eff} = 1.82–1.96 B.M., low spin d^5 S = ½), as is normal for ruthenium(II) and ruthenium(III) complexes, respectively [21] (Table 1).

*^1H NMR spectra of cis-$[Ru^{II}(bipy)_2L](PF_6)$ (**1a–b**) and cis-$[Ru^{II}(bipy)_2L](PF_6)_2$ (**1c**) complexes*

The ^1H NMR spectra is a good tool to check the purity of organic compounds. The ^1H NMR spectra of the ruthenium(II) complexes (**1a–c**) were recorded in DMSO-d_6. Due to the similarity of the aromatic protons signals they all appear in a narrow range. The signals of the aromatic protons appeared as a multiple in the spectra of the ligands and complexes within the range 8.20–7.00 ppm. However, the intensity measurements correspond accurately to the total number of aromatic protons in these complexes. An isolated signal was observed within the range 5.20–4.80 ppm and this signal was assigned to the amino group protons of the ligands.

Infrared spectra

The IR spectral data of the organic ligands and their Ru complexes are compared and the following features can be pointed out:

(1) The broad and medium intensity band due to υ(OH) group which appear in the spectra of the free ligands 2-aminophenol and 8-hydroxyquinoline at 3430–3390 cm^{-1} region were shifted to lower wavenumbers by 5–12 cm^{-1} upon complexation denoting its coordination to Ru center through deprotonated hydroxyl group of 2-aminophenol and 8-hydroxyquinoline [16].

Table 1
Electronic spectral data and ligand field parameters[a] (cm^{-1}) for the prepared complexes in DMF.

Ru(II) complexes	$ν_1(^1A_{1g} \to {}^1T_{1g})$	$ν_2(^1A_{1g} \to {}^1T_{2g})$	$ν_3(^1A_{1g} \to {}^1E_{1g})$ π–π*, n–π*	$ν_2/ν_1$	Δ_o	*B*	*C*	*β*
1a	17,825	25,595	40,322	1.43	17,800	712	3166	0.73
1b	17,825	25,706	30,387	1.44	18,564	714	3175	0.75
1c	17,141	25,316	35,087	1.47	18,080	630	2802	0.65
Ru(III) complexes	$ν_1(^2T_{2g} \to {}^2A_{1g}, {}^2T_{1g})$	$ν_2(^2T_{2g} \to {}^2E_g)$	$ν_3(^2T_{2g} \to {}^2A_{1g})$ π–π*, n–π*	$ν_2/ν_1$	Δ_o	*B*	*C*	*β*
2a	18,519	23,095	30,030	1.25	20,820	694	3086	0.72
2b	17,649	23,529	29,070	1.33	23,397	709	3153	0.73
2c	17,035	22,222	25,445	1.30	20,820	694	3086	0.72

[a] The ligand field parameters (Δ_o, *B*, *C* and *β*) were calculated by data obtained from the experimental UV–visible spectra of the complexes and Tanabe–Sugano diagrams for d^6 and d^5 octahedral geometry [24].

(2) The two bands appearing at 3435 and 3334 cm^{-1} in the spectrum of 2-aminophenol which correspond to $\upsilon_{as}(NH_2)$ and $\upsilon_s(NH_2)$ were shifted to lower wavenumbers at (3325 and 3285 cm^{-1}) and (3320 and 3280 cm^{-1}) in the Ru complexes (**1a**) and (**2a**), respectively, indicating that the NH_2 groups are taking part in coordination to the Ru center [17].

(3) In complexes **1c** and **2c** the bands due to $\upsilon_{as}(NH_2)$ and $\upsilon_s(NH_2)$ and $\upsilon(CO)$ were shifted to lower wavenumbers at 3315, 3242 and 1660 cm^{-1}) and (3315, 3242 and 1670 cm^{-1}), respectively, indicating their coordination to the Ru center. These results are similar to the recently reported bands in the complex $[Mn(NCS)_2(4\text{-}apy)_2]$ [22].

(4) For the Ru(III) complexes (**2a–c**), a strong single band was observed at 330 cm^{-1} assignable to the Ru—Cl group and absent in the Ru(II) complexes (**1a–c**) [23].

(5) Another weak bands were observed in the 470–455 and 450–435 cm^{-1} regions can be assigned to υ(Ru—O) and υ(Ru—N), respectively, confirming the coordination of both oxygen and nitrogen atoms to Ru center [23].

(6) The two bands appearing near 845 and 830 cm^{-1} in the Ru(II) complexes (**1a–c**) corresponding to υ(P—F) stretching vibration [24].

Electronic spectra of complexes

The electronic spectra of all complexes are recorded in DMF solvent in the range 300–700 nm. The spectral data are listed in Table 1 and a representative spectrum is shown in Fig. 1. The ground state of ruthenium(III) ion (t_{2g}^5 configuration) is $^2T_{1g}$ and the first excited doublet levels in order of increasing energy are $^2A_{2g}$ and $^2T_{1g}$ which arise from the $t_{2g}^4\,e_g^1$ configuration. These ruthenium(III) complexes are low spin (t_{2g}^5) with one unpaired electron; thus the bands observed can assigned to ligand field transitions for ruthenium(III) with a (t_{2g}^5) configuration. The electronic spectra of these complexes are similar and displayed three mean bands. According to Tanabe–Sugano energy matrices [25] for d^5-octahedral geometry, The bands observed in the range of 17,035–18,519 and 22,222–23,529 cm^{-1} are assigned to $^2T_{2g} \rightarrow {}^2A_{1g}$ or $^2T_{1g}$ and $^2T_{2g} \rightarrow {}^2E_g$ transitions, respectively. Bands of high intensity in the range of 25,445–30,864 cm^{-1} are also observed, these bands are attributed to π–π^* and n–π^* intra-ligand charge transfer. The ligand field parameters can be estimated by using the energies $^2T_{2g} \rightarrow {}^2A_{1g}$ and/or $^2T_{1g}$ and $^2T_{2g} \rightarrow {}^2E_g$ transitions, and the Tanabe–Sugano energy matrices for d^5-octahedral geometry [25]. We found that the splitting parameter, Δ_o in the range of 20,820–23,397 cm^{-1}, the Racah parameter of interelectronic repulsion, B in the range of 685–709 cm^{-1}, and the nephelauxetic ratio, β in the range 0.65–0.75. These values are close to those reported for similar octahedral ruthenium(III) complexes [26].

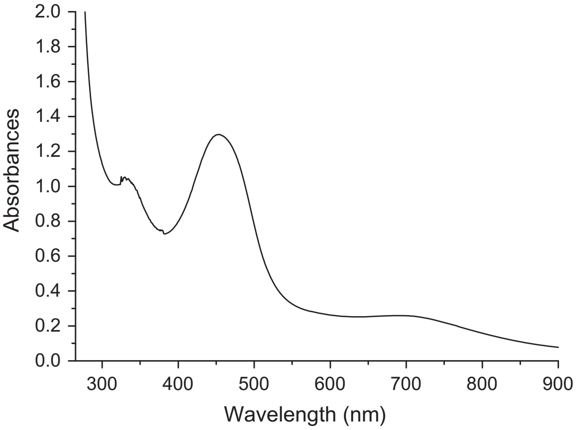

Fig. 1. Electronic spectrum of cis-$[Ru^{II}(bpy)_2(2\text{-}aph)](PF_6)$ (**1a**) in DMF.

The electronic spectra of the ruthenium(II) complexes are similar and display absorption bands in the regions 17,141–17,825, 25,316–25,706 and 30,387–40,322 cm^{-1}. The first two bands are attributable to $^1A_{1g} \rightarrow {}^1T_{1g}$ and $^1A_{1g} \rightarrow {}^1T_{2g}$ transitions, respectively, while the third high energy band is assigned to $^1A_{1g} \rightarrow {}^1E_{1g}$ transition [26,27]. Similarly, the ligand field parameters for ruthenium(II) complexes can be estimated. However, the values of ligand field parameters (Δ_o, B and β) are in the range of 17,800–19,080 630–714 and 0.72–0.73 respectively. The values are slightly close to those reported [28]. These values of the splitting parameters placed the ligands in the middle range of the spectrochemical series and provide reassurance that these ligands are coordinated to the ruthenium(II) ions through the oxygen atom of deprotonated hydroxyl group and nitrogen atom of the amino group. The value of B for ruthenium(II) complexes also indicates a considerable overlap with strongly covalent metal–ligand bond [29,30]. Electronic spectrum of cis-$[Ru^{II}(bpy)_2(2\text{-}aph)](PF_6)$ (**1a**) is shown in Fig. 1 as representative example.

*ESR spectra of $[Ru^{III}Cl(L)_2(H_2O)]$ (**2a–b**) and $[Ru^{III}Cl_2(L)_2]Cl$ (**2c**) complexes*

The complexes $[Ru^{III}Cl(L)_2(H_2O)]$ (**2a–b**) and $[Ru^{III}Cl_2(L)_2]Cl$ (**2c**) are one electron paramagnetic species (low spin d^5, S = ½). This confirms the +3 oxidation state of ruthenium. The ESR spectral data are listed in Table 2 and one representative example of their spectra (Fig. 2). The spectra of these solid complexes were similar and recorded in DMF/Toluene at 77 K. The spectra of all the complexes showed no hyperfine splitting. By ignoring the non-planarity of the carbon atoms, relative to the coordinated oxygen and nitrogen atoms of the ligands, a D_{2h}-symmetry for the complexes is suggested in which the coordinated chlorides are passing through the Z-axis while the coordinated oxygen and nitrogen atoms of the ligands pass through X and Y axes as shown in Scheme 2. In

Table 2
Magnetic, ESR and cyclic voltammetric data[a] for cis-$[Ru^{II}(bpy)_2L]^+$ (**1a–b**), cis-$[Ru^{II}(bpy)_2L]^{2+}$ (**1c**) and $[Ru^{III}Cl(L)_2(H_2O)]$ (**2a–b**) $[Ru^{III}Cl_2(L)_2]Cl$ (**2c**) complexes (L = 2-aph, 8-hq and 4-apy).

Complex	μ_{eff} (B.M.)	$g_{\parallel}$	$g_{\perp}$	E_{pa}(mV)	E_{pc} (mV)	ΔE (mV)	Assignment (reduction)	E_{pa} (mV)	E_{pc} (mV)	ΔE (mV)	Assignment (oxidation)	Scan rate ($mV\,s^{-1}$)
1a	0	–	–	–	–	–	–	550	440	110	Ru(II)/Ru(III)	50
1b	0	–	–	–	–	–	–	380	310	70	Ru(II)/Ru(III)	50
1c	0	–	–	–	–	–	–	390	320	70	Ru(II)/Ru(III)	50
2a	1.93	2.35	2.35	−740	−820	80	Ru(III)/Ru(II)	660	–	–	Ru(III)/Ru(IV)	50
2b	1.82	2.38	2.32	−600	−675	75	Ru(III)/Ru(II)	400	–	–	Ru(III)/Ru(IV)	50
2c	2.02	2.40	2.36	−290	−360	70	Ru(III)/Ru(II)	950	–	–	Ru(III)/Ru(IV)	50

[a] *Conditions:* supporting electrolyte (0.1 M tetrabutylammonium chloride in DMF solvent), concentration of the complex (6×10^{-3} M), $\Delta E = E_{pa} - E_{pc}$ and $E_{1/2} = 0.5(E_{pa} + E_{pc})$, where E_{pa} and E_{pc} are the anodic and cathodic cyclic voltammetric peak potentials, respectively.

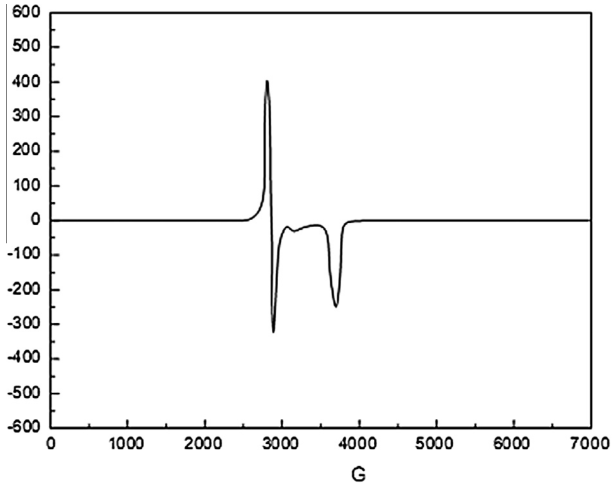

Fig. 2. ESR spectrum of $[Ru^{III}Cl(2\text{-}aph)_2(H_2O)]$ (**2a**) in DMF/toluene at 77 K.

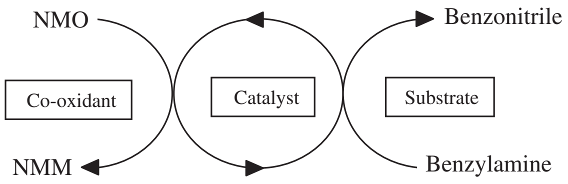

Scheme 2. Catalytic cycle for dehydrogenation of benzylamine to benzonitrile.

view of the suggested stereochemistry of these complexes, it was found that they showed tetragonal ESR spectra with two distinct g-values. The first signal was found near 2.40–2.35 ($g_{||}$ in the axial case) and the second near 1.98–1.78 (rhombic component of $g_{\perp}$). The presence of two g values is an indication of an octahedral field with tetragonal distortion ($g_x \neq g_y \neq g_z$) and also points out an axial symmetry for the complexes and hence trans positions are assigned for the two chlorides ligand in the case of $[Ru^{III}Cl_2(L)_2]Cl$ (**2c**) complex (Fig. 2). This assignment is in conformity with the assignment made for similar octahedral ruthenium(III) complexes [31].

Electrochemical studies

The electrochemical properties of all complexes have been investigated by using cyclic voltammetry in DMF (6×10^{-3} M) and supporting electrolyte (0.1 M) tetrabutylammonium chloride (TBAC). Voltammetric data are presented in Table 2 and selective voltammograms are shown in Fig. 3. All ruthenium(II) complexes show one reversible oxidation wave (ΔE = 60–110 mV) on the positive side and this wave assigned to Ru(II)/Ru(III) oxidation. The anodic peak current (i_{pa}) and the cathodic peak current (i_{pc}) are almost equal. Under the same conditions ruthenium(III) complexes show one reversible reduction wave (ΔE = 70–80 mV) on the negative side against Ag/AgCl and irreversible oxidation peak (E_{pa} = 380–950 mV) on the positive side. The former is assigned to Ru(III)/Ru(II) reduction and the latter is assigned to Ru(III)/Ru(IV) oxidation. The one electron nature of these waves was confirmed by comparing the peak heights for each wave with that of the ferrocene–ferrocenium couple under the same conditions (Fig. 3).

Catalytic dehydrogenation of aromatic amines to nitriles

Attempts to dehydrogenate benzyl amine, *p*-methyl benzylamine and *p*-nitrobenzylamine by cis-$[Ru^{II}Cl_2(bpy)_2]\cdot 2H_2O$/*N*-methylmorpholine-*N*-oxide (NMO) catalyst system to their corresponding nitriles were all unsuccessful since an unidentified product was found at the end, probably due to the degradation of aromatic ring by cis-$[RuCl_2^{II}(bpy)_2]\cdot 2H_2O$ complex [32]. The two complexes, cis-$[Ru^{II}(bpy)_2(8\text{-}hq)](PF_6)$ (**1b**) and $[Ru^{III}Cl(8\text{-}hq)_2$

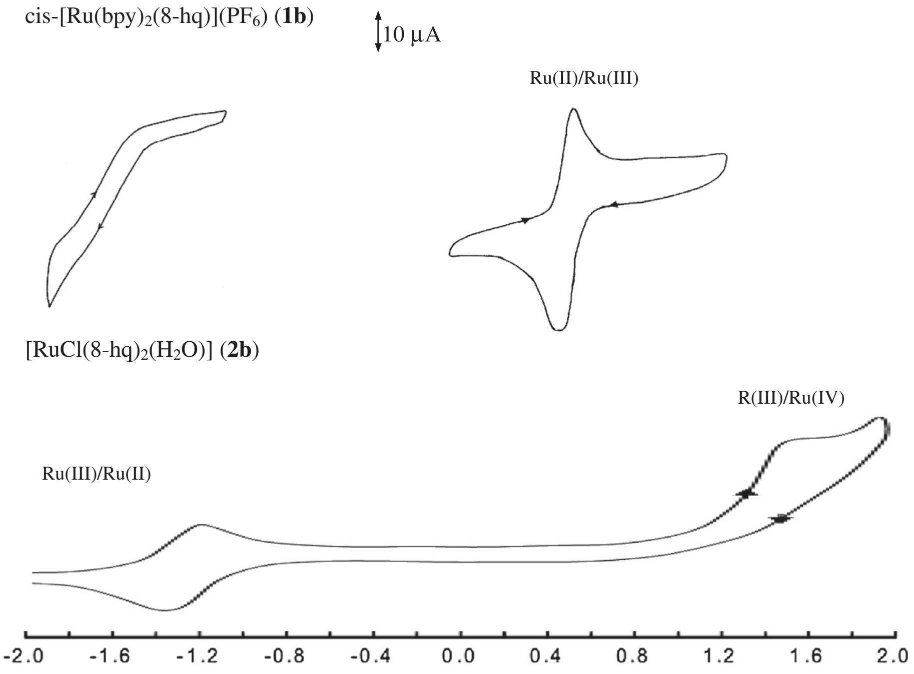

Fig. 3. Cyclic voltammograms of the complexes: cis-$[Ru^{II}(bpy)_2(8\text{-}hq)](PF_6)$ (**1b**) and $[Ru^{III}Cl(8\text{-}hq)_2(H_2O)]$ (**2b**). Concentration = 6×10^{-3} M in 0.1 M tetrabutylammonium chloride DMF solution) at scan rate 50 mV s^{-1}.

Table 3
Optimum conditions for catalytic dehydrogenation of R—PhCH$_2$—NH$_2$ to R—PhCN (R = H, *p*-CH$_3$ and *p*-NO$_2$).

Entry	Solvent	Temp (°C)	Time (H)	Yield (%) cis-[Ru^{II}(bipy)$_2$(8-hq)](PF$_6$) (**1b**)			Yield (%) [Ru^{III}Cl(8-hq)$_2$(H$_2$O)] (**2b**)		
				H	*p*-CH$_3$	*p*-NO$_2$	H	*p*-CH$_3$	*p*-NO$_2$
1	Dioxane	25	5	25	24	30	31	36	35
2	THF	25	5	22	33	36	27	35	36
3	CH$_2$Cl$_2$	25	5	20	22	25	26	27	33
4	DMF	25	3	63	63	60	70	68	71
5	DMF	40	2	88	85	86	95	91	88

(H$_2$O)] (**2b**) were examined as catalysts instead of cis-[Ru^{II}Cl$_2$(bpy)$_2$]·2H$_2$O for catalytic dehydrogenation of these substrates.

The catalytic dehydrogenation reaction occurs according the following equation:

$$\text{R—Ph—CH}_2\text{NH}_2 + 2\text{NMO} \xrightarrow[\text{R=H, } p\text{-Methyl and } p\text{-Nitro}]{\text{Ru-catalyst, DMF}} \text{R—Ph—CN} + 2\text{NMM} + 2\text{H}_2\text{O}$$

Our preliminary results are summarized in Table 3. In order to establish the optimum conditions for catalytic dehydrogenation of these substrates we studied the influence of solvent on these oxidations was investigated. In CH$_2$Cl$_2$, dioxane, THF and DMF, low yields of nitriles were obtained with CH$_2$Cl$_2$, dioxane, and THF (Table 3, entries 1–3) and dramatic increase in the yields from 36% to 71%, however, were obtained in DMF (Table 3, entry 3 and 4) which was therefore used as the solvent in all other experiments. Next, the effect of temperature was examined. Increasing the temperature from 25 to 40 °C resulted in a considerable increase in the yield and shorter reaction times (Table 3, entry 5). It was found that yields obtained with the ruthenium(III) complex are slightly higher than whose obtained with the ruthenium(II) complex, probably due to the +3 oxidation state of the ruthenium(III) enhances the oxidation reactions more the +2 oxidation state of ruthenium(II) complex.

In a typical experiment, a DMF solution of an excess amount of NMO (3 mmol) was added to a stirred solution of benzylamine (2 mmol) and a catalytic amount of the complex (**1b** or **2b**) (0.01 mmol). After stirring for 15 min the reaction mixture turned to dark brown, probably due to the coordination of benzylamine to ruthenium center as had been reported by Griffith and co-workers [19]. Therefore, we suggest that the catalytic dehydrogenation of primary amines has been promoted by their coordination to ruthenium center. Unfortunately our attempt to isolate the produced benzylamine complex in this work was unsuccessful.

A blank experiments were carried out under the same conditions, we observed that the yields of nitriles obtained in the absence of the catalyst is less than 5%; this reflects the role of the ruthenium catalyst in the catalytic oxidation reactions. The most commonly proposed mechanism for dehydrogenation of benzylamine by low-valent ruthenium complexes involves the formation of a ruthenium-oxo intermediate by reaction of *N*-methylmorpholine-*N*-oxide (NMO) with the ruthenium center. Benzylamine coordinates to this intermediate which is coordinatively saturated. However, the produced benzylamine-ruthenium complex is converted into Ru-imine-complex through a β-hydrogen elimination step from the coordinated benzylamine with removal of an H$_2$O molecule. The produced ruthenium-imine complex is further dehydrogenated by the same way to give benzonitrile, another H$_2$O molecule, *N*-methylmorpholine (NMM) and the original ruthenium complex. Although further investigation of the mechanistic details is needed, we believe that the ruthenium-oxo intermediate complexes enhance the elimination of hydrogen from the coordinated benzylamine. This catalytic cycle will continue until all the benzylamine is completely dehydrogenated as shown in Scheme 2. Similar mechanistic study was suggested for dehydrogenation of benzylamine by [RuCl(ppy)(tpy)] (ppy = 2-phenylpyridine and tpy = 2,2′:6′,2″-terpyridine) with molecular oxygen as co-oxidant [33]. In conclusion, we have developed an efficient method for catalytic oxidation of these amines to nitriles by these two complexes. Attempts to dehydrogenate some aliphatic amines are in progress.

Conclusion

Two series of ruthenium complexes, cis-[Ru^{II}(bpy)$_2$L](PF$_6$) (**1a–b**), cis-[Ru^{II}(bpy)$_2$L](PF$_6$)$_2$ (**1c**) and [Ru^{III}Cl(L)$_2$(H$_2$O)] (**2a–b**) [Ru^{III}Cl$_2$(L)$_2$]Cl (**2c**) have been synthesized and characterized by several physicochemical techniques. The spectroscopic analysis (IR, UV–Vis, ^{1}H NMR, ESR) of these complexes indicates an octahedral geometry for all the complexes. Cyclic voltammograms of ruthenium(II) complexes exhibit one reversible oxidation wave on the positive side attributable to Ru(II)/Ru(III) reduction, while ruthenium(III) complexes exhibit one reversible reduction wave on the negative side against Ag/AgCl, and irreversible oxidation peak on the positive side. The former is assigned to Ru(III)/Ru(II) reduction and the latter is assigned to Ru(III)/Ru(IV) oxidation. The complexes, cis-[Ru^{II}(bpy)$_2$(8-hq)](PF$_6$) (**1b**) and [Ru^{III}Cl(8-hq)$_2$(H$_2$O)] (**2b**) dehydrogenate benzylamine, *p*-methylbenzylamine and *p*-nitrobenzylamine to their respective nitriles in DMF as a solvent and in the presence of *N*-methylmorpholine-*N*-oxide (NMO) as co-oxidant in good yields and turnover.

References

[1] J. Wang, Y. Zhao, X. Jin, L. Yang, H. Wang, Spectrochim. Acta A 122 (2014) 649–655.
[2] A.A. Abdel Aziz, H.A. Elbadawy, Spectrochim. Acta A 124 (2014) 404–415.
[3] M. Shen, A.J. Bard, J. Am. Chem. Soc. 133 (2011) 15737–15742.
[4] P.P. Laine, S. Campagna, F. Loiseau, Coord. Chem. Rev. 252 (2008) 2552–2571.
[5] W.P. Griffith, Ruthenium oxidation complexes in catalysis by metal complexes, Springer Sci. 34 (2011) 227–228.
[6] S.A. Moya, J.C. Araya, J. Gajardo, V. Guerchais, H. Le Bozec, L. Toupet, P. Aguirre, Inorg. Chem. Commun. 27 (2013) 108–110.
[7] S.K. Sarkar, M.S. Jana, T.K. Mondal, C. Sinha, J. Organomet. Chem. 716 (2012) 129–137.
[8] J.G. Małecki, A. Maron, S. Krompiec, M. Filapek, M. Penkala, B. Marcol, Polyhedron 49 (2013) 190–199.
[9] F. Li, J. Chen, Q. Zhang, Y. Wang, Green Chem. 10 (2008) 553–562.
[10] N. Miyaura, Synlett 13 (2009) 2039–2050.
[11] F. Chen, Z. Peng, H. Fu, J. Liu, L. Shao, J. Chem. Res. (S) 12 (1999) 726–727.
[12] K. Yamaguchi, N. Mizuno, Angew. Chem., Int. Ed. 42 (2003) 1480–1483.
[13] J.S.M. Samec, A.H. Ell, J.E. Backvall, Chem. Eur. J. 11 (2005) 2327–2334.
[14] A.F. Shoair, J. Coord. Chem. 60 (2007) 1101–1109.
[15] A.F. Shoair, R.H. Mohamed, J. Coord. Chem. 60 (2007) 1279–1289.
[16] A.Z. El-Sonbati, M.A. Diab, A.A. El-Bindary, M.I. Abou-Dobara, H.A. Seyam, Spectrochim. Acta A 104 (2013) 213–221.
[17] M.A. Diab, A.Z. El-Sonbati, A.A. El-Bindary, A.M. Barakat, Spectrochim. Acta A 116 (2013) 428–439.
[18] A.F. Shoair, Bull. Korean Chem. Soc. 26 (2005) 1525–1528.
[19] W.P. Griffith, B. Reddy, A.F. Shoair, M. Suriaatmaja, A.J.P. White, D.J. Williams, J. Chem. Soc., Dalton Trans. (1998) 2819–2825.
[20] B.P. Sullivan, D.J. Salmon, T.J. Meyer, Inorg. Chem. 17 (1978) 3334–3341.
[21] I. Warad, M. Al-Noaimi, O.S. Abdel-Rahman, F.F. Awwadi, B. Hammouti, T.B. Hadda, Spectrochim. Acta A 117 (2014) 250–258.
[22] M.R. Saber, F.A. Mautner, J. Mol. Struct. 1020 (2012) 177–182.

[23] M. Milos, T. Penhouet, P. Pal, A. Hauser, Inorg. Chem. 49 (2010) 3402–3408.
[24] W. Man, H. Kwong, W.W.Y. Lam, J. Xiang, T.-W. Wong, W.-H. Lam, W.-T. Wong, S.-M. Peng, T.-C. Lau, Inorg. Chem. 47 (2008) 5936–5944.
[25] Y. Tanabe, S. Sugano, J. Phys. Soc. Jpn. 9 (1954) 753–766.
[26] R. Abu-Eittah, M.M. Hammed, Bull. Chem. Jpn. 57 (1984) 844–851.
[27] N.C. Pramanik, S. Bhattacharya, Polyhedron 16 (1997) 1755–1761.
[28] M.S. El-Shahawi, A.F. Shoair, Spectrochim. Acta A 60 (2004) 121–127.
[29] L.D. Field, B.A. Messerle, L. Soler, I.E. Buys, T.W. Hambley, J. Chem. Soc., Dalton Trans. (2001) 1959–1965.
[30] A.B.P. Lever, Inorganic Electronic Spectroscopy, second ed., Elsevier, Amsterdam, 1984.
[31] P.S. Chittilappilly, K.M. Yusuff, Indian J. Chem. 47A (2008) 848–853.
[32] A.K. Chakraborti, U.R. Ghatak, J. Chem. Soc., Perkin Trans. (1985) 2605–2609.
[33] A. Taketoshi, T. Koizumi, T. Kanbara, Tetrahedron Lett. 51 (2010) 6457–6459.